In situ observation of rapid reactions in nanoscale Ni–Al multilayer foils using synchrotron radiation

Konrad Fadenberger,[1,2] Ibrahim Emre Gunduz,[1,a)] Chrysostomos Tsotsos,[1] Maria Kokonou,[1] Styliani Gravani,[1] Stefan Brandstetter,[3] Anna Bergamaschi,[3] Bernd Schmitt,[3] Paul H. Mayrhofer,[2] Charalabos C. Doumanidis,[1] and Claus Rebholz[1]
[1]*Department of Mechanical and Manufacturing Engineering, University of Cyprus, 1678 Nicosia, Cyprus*
[2]*Department of Physical Metallurgy and Materials Testing, Montanuniversität Leoben, A-8700 Leoben, Austria*
[3]*Paul Scherrer Institute, CH-5232 Villigen-PSI, Switzerland*

(Received 21 May 2010; accepted 13 August 2010; published online 5 October 2010)

The observation of rapid reactions in nanoscale multilayers present challenges that require sophisticated analysis methods. We present high-resolution *in situ* x-ray diffraction analysis of reactions in nanoscale foils of $Ni_{0.9}V_{0.1}$–Al using the Mythen II solid-state microstrip detector system at the Material Science beamline of the Swiss Light Source Synchrotron at Paul Scherrer Institute in Villigen, Switzerland. The results reveal the temperature evolution corresponding to the rapid formation of NiAl intermetallic phase, vanadium segregation and formation of stresses during cooling, determined at high temporal (0.125 ms) and angular (0.004°) resolution over a full angular range of 120°. © *2010 American Institute of Physics*. [doi:10.1063/1.3485673]

Self-propagating exothermic reactions (SPER) in nanoscale multilayer films/foils (MFs) of metallic systems are receiving attention as heat sources for micromesoscale robotics/self autonomous devices and for thermal nanomanufacturing.[1–15] The actual reaction route for MFs has remained elusive, because high flame front velocities (1–20 m/s) require highly sophisticated *in situ* characterization methods, such as dynamic transmission electron microscopy (DTEM) (Ref. 16) and synchrotron radiation.[13]

However, DTEM analysis is restricted to very thin foils (~125 nm) for which the convective heat losses are very significant and the analysis cannot adequately represent the kinetics of microscale foils. Previous work using synchrotron radiation was performed on $Ni_{0.36}V_{0.04}$–$Al_{0.6}$ MFs with a bilayer thickness of 100 nm.[13] Despite the high temporal resolution (0.055 ms), the x-ray diffraction (XRD) patterns lack the necessary angular resolution to accurately identify phases.[13] Therefore, we have performed *in situ* XRD analysis of rapid reactions in nanoscale MFs of $Ni_{0.9}V_{0.1}$–Al with a bilayer thickness of 40 nm at an angular resolution of 0.004° and a temporal resolution of 0.125 ms using the recently modified Mythen II solid-state micro strip detector system at the Material Science (X04SA) beamline of the Swiss Light Source at Paul Scherrer Institute in Villigen, Switzerland, in combination with high-speed (HS) optical and infrared (IR) imaging. A detailed description of the previous model of the detector system[17] and an overview of the current version[18] was published elsewhere. The system allows the monitoring of evolution of nanoscale structures, temperature and strain variations, with time resolution of submilliseconds at unsurpassed angular accuracy and range, which is ideal for the observation of the transient characteristics of SPER in MFs. The setup used in this study and the transmission electron microscopy (TEM) image of the cross section of the foil in the as-received state are shown in Fig. 1.

60 μm thick foils with an overall composition $Ni_{0.9}V_{0.1}$ (16 nm)-Al (24 nm) are obtained from Reactive Nano Technologies Inc.©. The source of vanadium is the nonmagnetic commercially available $Ni_{0.9}V_{0.1}$ sputtering targets used, which are also employed in cd/dvd production. The surfaces of the foils are polished to remove the INCUSIL© solder layer. The detector system is operated in transmission geometry at 14 keV beam energy. The acquisition times of 0.125, 0.25, 1, and 5 ms have 0.125 and 20 ms dead time between frames, which are imposed by the controller memory and data transfer rate in conjunction with the chosen dynamic range. The analyzed volume is $500 \times 500 \times 55$ μm^3. Foils of 7×25 mm^2 size are ignited by a high-voltage electric spark. Simultaneously, HS optical camera (MEGA SPEED Corporation MS70K DMG2© up to 80 000 frames/s) and IR

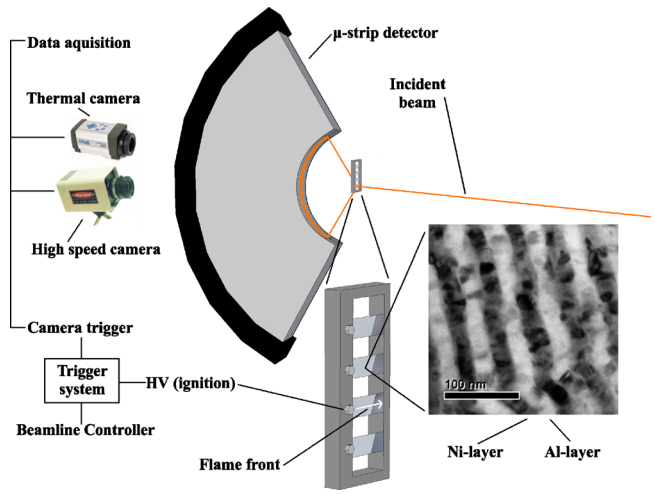

FIG. 1. (Color online) The experimental setup: the Mythen II solid state detector has an angular range of 120° (2θ from −60° to 60°) at a resolution of 0.004°. The central trigger system provides a high-voltage spark to the sample holder and generates a start trigger for the signal generator for the beamline controller and the cameras. The inset shows a bright field TEM micrograph of the initial multilayer structure.

a)Electronic mail: emreth@ucy.ac.cy.

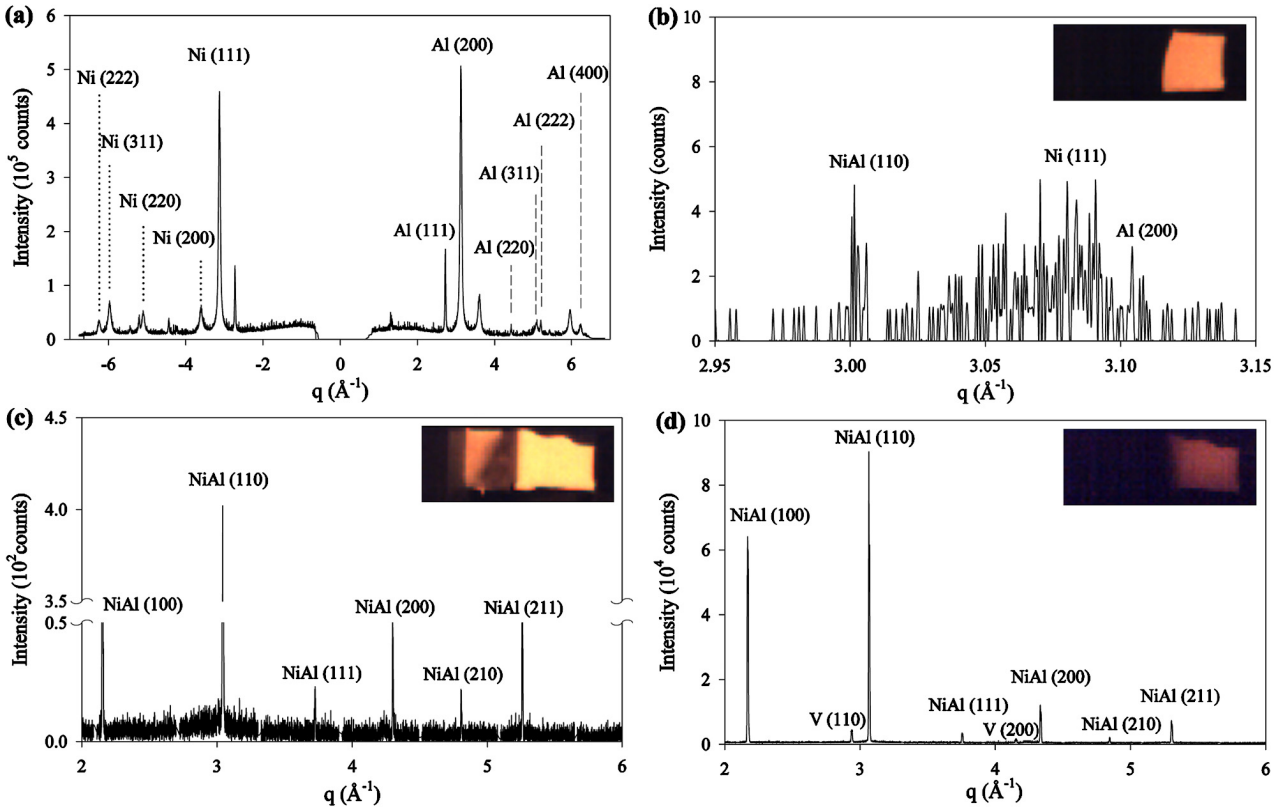

FIG. 2. (Color online) XRD pattern with the corresponding HS optical images: (a) The overall pattern (2θ from $-60°$ to $60°$) before the reaction, where broadened peaks of $Ni_{0.9}(V_{0.1})$ and Al correspond to grain sizes of 7.5 and 24 nm, (b) 1 to 1.125 ms after ignition showing superposed peaks of reactants in their initial state and NiAl that has formed ($T=1900\pm30$ K), (c) 8 to 9 ms after ignition ($T=1900\pm30$ K), and (d) 260 to 265 ms after ignition, when formation of vanadium and solid NiAl from the remaining liquid through the pseudoeutectic reaction is complete ($T=1700\pm35$ K).

camera (FLIR Systems THERMOVISION A40M© at 50 frames/s) images are acquired. As time reference, the trigger signals for the XRD detector are recorded. The multilayer structures were characterized using TEM (PHILIPS CM20©), scanning electron microscopy (SEM, TESCAN VEGA©) and optical microscopy. The grain sizes and the strains are determined using the Williamson–Hall method. The changes in lattice parameters are used to measure temperature with a thermal expansion coefficient of 15×10^{-6} K^{-1} for NiAl.

Diffraction patterns taken before the reaction [Fig. 2(a)] show broad peaks of nanoscale FCC nickel and aluminum grains with average sizes 7.5 nm and 24 nm, respectively. Following ignition, the thermal wave quickly traverses the foil at a velocity ~7.3 m/s (Refs. 3, 5, 6, and 14) and arrives at the irradiated volume after ~1 ms. The measured temperature is 1900 ± 30 K within the first XRD frame [Fig. 3(a)], 0.125 ms after the thermal wave passes, which shows the superimposed peaks from nickel and aluminum bilayers, as well as that from NiAl that shifts to lower angles as the lattice expands with increasing temperature [Fig. 2(b)]. The maximum temperature is close to the theoretical room temperature adiabatic formation temperature of 1911 K for NiAl, at which a mixture of solid with a thickness of ~22 nm and liquid should coexist.[19] Numerical simulations performed for a bilayer thickness of 40 nm using an adiabatic growth model[15] agree with the measured temperature evolution [Fig. 3(a)]. Therefore SPER appears to proceed in a near-adiabatic manner for foils of this thickness, in contrast to studies with thinner foils,[16] which have a larger surface area per reacting volume, as well as to foils with a different overall composition (Ni_2Al_3) that do not reach temperatures higher than 1700 K.[13]

The full width half maximum ($\Delta2\theta_{fwhm}$) for the NiAl peak measured at a frame time of 0.25 ms is ~0.045°–0.05°. The NiAl grains are most possibly in the form of platelets with a thickness 25 ± 3 nm and a length of at least 115 ± 5 nm indicating that the reactants transform completely into NiAl within this frame. The main NiAl peak is accompanied by a pronounced background and suggests the formation of the liquid phase as well when observed at a 1 ms frame time [Fig. 2(c)].

The temperature remains steady for 60 ms and decreases slowly in the following 160 ms, during which the liquid continues to solidify with a corresponding increase in NiAl peak intensity. Solid vanadium peaks appear in the spectra at around $\sim1700\pm35$ K, which is near the reported pseudobinary eutectic temperature (1635 K),[20] followed by a drop in background intensity [Fig. 2(d)]. The inflection point at the time-temperature profile [Fig. 3(a)] suggests that solidification of the liquid is complete. The foil cools down to room temperature within ~10 s. A simple theoretical calculation with convective and radiative heat losses, using a temperature-dependent convection coefficient of air[21] and $\varepsilon=0.11$, fits very well with the measured cooling curve.

The microstructure of the foils shows equiaxed NiAl grains with an average diameter of 3 μm [Figs. 3(b) and 3(c)], which are uniformly distributed across the thickness. Vanadium grains are within the NiAl grain boundaries and have an average diameter of 50 ± 5 nm, measured using peak widths and SEM [Fig. 3(b), inset]. Comparison between

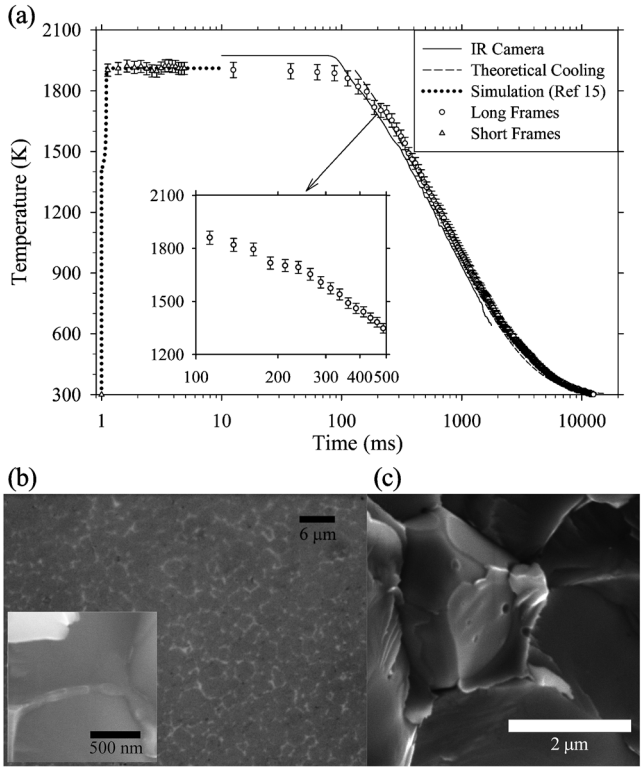

FIG. 3. (a) Temperatures are measured using the NiAl peak locations with short (acquisition times 0.125, 0.25, and 1 ms, dead time 0.125 ms) and long frames (acquisition time 5 ms, dead time 20 ms), the IR camera and calculated using simple theoretical cooling curve and simulation results assuming an adiabatic reaction. The time axis is relative to ignition time, the flame front reaches the analyzed volume at 1 ms. (b) Optical micrograph showing the vanadium phase within the NiAl grain boundaries across the foil cross section. The inset is a high magnification SEM image of the grain boundary. (c) Highly stressed vanadium grain boundary phase that appears as a thin layer on the NiAl grain, acts as crack nucleation site during intergranular fracture of foils.

the change of lattice parameters of vanadium and NiAl during cooling using corresponding thermal expansion coefficients,[22] implies that vanadium grains are under increasing tensile stress due to the higher thermal expansion coefficient of the surrounding NiAl matrix. The calculated strains are around 0.2%. Similar phenomena have been observed in molybdenum nanowires that were embedded in NiAl matrix, which contract at a rate close to that of NiAl during cooling.[23] The fact that vanadium is still in grain boundaries after the foil cools down indicates that NiAl grains reach their final size when vanadium forms between 220–260 ms.

We propose that the grain evolution starts with the formation of NiAl platelets with high aspect ratios. These initial grains break up when the maximum temperature is reached due to the rapid growth of NiAl, also evidenced by the bulk warping of the foils. The fragments spherodize in the liquid and the NiAl grains continue to grow into the liquid solution consisting of NiAl and vanadium until the solidification is finished at $\sim 1700 \pm 35$ K. No shape changes of the foils are observed after 20 ms.

In summary, observation of SPER on nanoscale structures reveal that the reaction stages, strains and grain dimensions can be identified and measured *in situ* during the rapid formation of intermetallic compound NiAl using the fast acquisition mode of the Mythen II x-ray microstrip detector system, in combination with HS optical and IR camera imaging. These experimental results are important for further validation of numerical models regarding temperature and structure development in $Ni_{0.9}V_{0.1}$–Al multilayer foils, as well as other metallic reactive systems.

We gratefully acknowledge the financial support from the FP6 Marie Curie Actions (Project Nos. EXT-0023899-NanoHeaters, EXC-006680–UltraNanoMan, and IP-026467–ManuDirect) of the European Commission, Cyprus Research Promotion Foundation-NanoCyprus and Paul Scherrer Institute for X04SA beamline access at the Swiss Light Source in February 2008 (#20070874), October 2008 (#20080434), and September 2009 (#20090387). This research project has been supported by the European Commission under FP6: Strengthening the European Research Area, Research Infrastructures (Project No. RII3-CT-2004-506008). Furthermore we would like to thank Dr. K. Giannakopoulos of IMS/NCSR Demokritos Athens, Greece for the TEM analysis.

[1]E. Ma, C. V. Thompson, L. A. Clevenger, and K. N. Tu, Appl. Phys. Lett. **57**, 1262 (1990).
[2]T. S. Dyer, Z. A. Munir, and V. Ruth, Scripta Met. et Mat. **30**, 1281 (1994).
[3]A. B. Mann, A. J. Gavens, M. E. Reiss, D. V. Heerden, G. Bao, and T. P. Weihs, J. Appl. Phys. **82**, 1178 (1997).
[4]D. V. Heerden, A. J. Gavens, S. Jayaraman, and T. P. Weihz, in *Phase Transformations and Systems Driven Far From Equilibrium*, MRS Symposia Proceedings No. 481, edited by E. Ma, P. Bellon, M. Atzmon, and R. Trivedi (Materials Research Society, Pittsburgh, 1998), pp. 533–538.
[5]S. Jayaraman, O. M. Knio, A. B. Mann, and T. P. Weihs, J. Appl. Phys. **86**, 800 (1999).
[6]A. J. Gavens, D. V. Heerden, A. B. Mann, M. E. Reiss, and T. P. Weihs, J. Appl. Phys. **87**, 1255 (2000).
[7]S. Jayaraman, A. B. Mann, M. Reiss, T. P. Weihs, and O. M. Knio, Combust. Flame **124**, 178 (2001).
[8]E. Besnoin, S. Cerutti, O. M. Knio, and T. P. Weihs, J. Appl. Phys. **92**, 5474 (2002).
[9]A. J. Swiston, Jr., T. C. Hufnagel, and T. P. Weihs, Scr. Mater. **48**, 1575 (2003).
[10]J. Wang, E. Besnoin, A. Duckham, S. J. Spey, M. E. Reiss, O. M. Knio, M. Powers, M. Whitener, and T. P. Weihs, Appl. Phys. Lett. **83**, 3987 (2003).
[11]J. Wang, E. Besnoin, A. Duckham, S. J. Spey, M. E. Reiss, O. M. Knio, and T. P. Weihs, J. Appl. Phys. **95**, 248 (2004).
[12]A. Duckham, S. J. Spey, J. Wang, M. E. Reiss, T. P. Weihs, E. Besnoin, and O. M. Knio, J. Appl. Phys. **96**, 2336 (2004).
[13]J. C. Trenkle, L. J. Koerner, M. W. Tate, S. M. Gruner, T. P. Weihs, and T. C. Hufnagel, Appl. Phys. Lett. **93**, 081903 (2008).
[14]I. E. Gunduz, K. Fadenberger, M. Kokonou, C. Rebholz, and C. C. Doumanidis, Appl. Phys. Lett. **93**, 134101 (2008).
[15]I. E. Gunduz, K. Fadenberger, M. Kokonou, C. Rebholz, C. C. Doumanidis, and T. Ando, J. Appl. Phys. **105**, 074903 (2009).
[16]J. S. Kim, T. LaGrange, B. W. Reed, M. L. Taheri, M. R. Armstrong, W. E. King, N. D. Browning, and G. H. Campbell, Science **321**, 1472 (2008).
[17]B. Schmitt, Ch. Broennimann, E. F. Eikenberry, F. Gozzo, C. Hoermann, R. Horisberger, and B. Patterson, Nucl. Instrum. Methods Phys. Res. A **501**, 267 (2003).
[18]A. Bergamaschi, Ch. Broennimann, R. Dinapoli, E. F. Eikenberry, F. Gozzo, B. Henrich, M. Kobas, P. Kraft, B. Patterson, and B. Schmitt, Nucl. Instrum. Methods Phys. Res. A **591**, 163 (2008).
[19]P. Zhu, J. C. M. Li, and C. T. Liu, Mater. Sci. Eng., A **357**, 248 (2003).
[20]J. D. Cotton, M. J. Kaufman, and R. D. Noebe, Scr. Metall. **25**, 1827 (1991).
[21]Y. Cengel, *Heat Transfer: A Practical Approach*, 2nd ed. (McGraw Hill, New York, 2003), p. 815.
[22]I. Barin, *Thermochemical Data of Pure Substances*, 3rd ed. (VCH, New York, 1995).
[23]H. Bei, E. P. George, D. W. Brown, G. M. Pharr, H. Choo, W. D. Porter, and M. A. M. Bourke, J. Appl. Phys. **97**, 123503 (2005).